BRAIN
ORIGINAL ARTICLE

Detection of neuron-derived pathological α-synuclein in blood

Annika Kluge,[1] Josina Bunk,[2] Eva Schaeffer,[1] Alice Drobny,[3] Wei Xiang,[3] Henrike Knacke,[1] Simon Bub,[3] Wiebke Lückstädt,[4] Philipp Arnold,[5] Ralph Lucius,[4] Daniela Berg[1,†] and Friederike Zunke[3,†]

[†]These authors contributed equally to this work.

To date, no reliable clinically applicable biomarker has been established for Parkinson's disease. Our results indicate that a long anticipated blood test for Parkinson's disease may be realized. Following the isolation of neuron-derived extracellular vesicles of Parkinson's disease patients and non-Parkinson's disease individuals, immunoblot analyses were performed to detect extracellular vesicle-derived α-synuclein. Pathological α-synuclein forms derived from neuronal extracellular vesicles could be detected under native conditions and were significantly increased in all individuals with Parkinson's disease and clearly distinguished disease from the non-disease state. By performing an α-synuclein seeding assay these soluble conformers could be amplified and seeding of pathological protein folding was demonstrated. Amplified α-synuclein conformers exhibited β-sheet-rich structures and a fibrillary appearance. Our study demonstrates that the detection of pathological α-synuclein conformers from neuron-derived extracellular vesicles from blood plasma samples has the potential to evolve into a blood-biomarker of Parkinson's disease that is still lacking so far. Moreover, the distribution of seeding-competent α-synuclein within blood exosomes sheds a new light of pathological disease mechanisms in neurodegenerative disorders.

1 Department of Neurology, University Hospital Kiel, 24105 Kiel, Germany
2 Institute of Biochemistry, Christian-Albrecht-University Kiel, 24118 Kiel, Germany
3 Department of Molecular Neurology, University Hospital Erlangen, Friedrich-Alexander University Erlangen-Nürnberg, 91054 Erlangen, Germany
4 Institute of Anatomy, Christian-Albrecht-University Kiel, 24118 Kiel, Germany
5 Institute of Functional and Clinical Anatomy, Friedrich-Alexander-University Erlangen-Nürnberg, 91054 Erlangen, Germany

Correspondence to: Annika Kluge
Department of Neurology
University Hospital Kiel
Arnold-Heller-Str. 3, 24105 Kiel, Germany
E-mail: annika.kluge@uksh.de

Correspondence may also be addressed to: Friederike Zunke
Department of Molecular Neurology
University Hospital Erlangen
Friedrich-Alexander University Erlangen-Nürnberg
Schwabachanlage 6, 91054 Erlangen, Germany
E-mail: friederike.zunke@fau.de

Keywords: α-synuclein; Parkinson's disease; biomarker; neuron-derived extracellular vesicles; seeding assay

Received October 28, 2021. Revised January 12, 2022. Accepted March 13, 2022

Abbreviations: α-syn = α-synuclein; DLS = dynamic light scattering; EV = extracellular vesicle; NCAM-L1 = neuronal cell adhesion molecule L1; NE = neuron-derived extracellular vesicle; TEM = transmission electron microscopy; ThT = Thioflavin T; UPDRS-III = Unified Parkinson's Disease Rating Scale Part 3

Introduction

Until now, the gold-standard to confirm Parkinson's disease is the post-mortem detection of misfolded α-synuclein (α-syn) as structural component of Lewy bodies in dopaminergic neurons in the substantia nigra.[1] However, in the clinical routine the diagnosis of Parkinson's disease is still based on the detection of motor symptoms, supported by imaging techniques and the assessment of concurrent non-motor symptoms and risk factors for Parkinson's disease.[2] Therefore, the correct diagnosis and appropriate therapy is still highly dependent on the professional experience of the examiner, and many epidemiological or post-mortem studies found high rates of misdiagnoses in Parkinson's disease.[3–6] Another major shortcoming of the clinical approach to diagnose Parkinson's disease is the substantially delayed identification of the disease, as the diagnosis-defining motor symptoms occur only late in the neurodegenerative process, i.e. when >50% of dopaminergic neurons in the substantia nigra have already been lost.[7] An earlier detection of the disease, ideally in the prodromal phase before motor symptoms occur, is of utmost importance for the development and application of disease-modifying therapies. Finally, the assessment of clinical symptoms by scales is still used as the primary outcome parameter in most clinical trials. This semi-quantitative approach is an imprecise reflection of actual disease progression, depending on a variety of potential confounders such as medication intake, examiner's experience and the physical as well as psychological form of the patient on the day of examination.

Taken together, there is an urgent need for an objective and reliable biomarker to improve the diagnostic accuracy of Parkinson's disease, detect the disease in early stages (preferably in the prodromal state) and monitor disease progression. In this respect, the detection of pathological α-syn as neuropathological hallmark of Parkinson's disease has been the centre of attention in a wide range of studies.[8] Many studies have focused on the identification of α-syn in accessible peripheral tissues for instance biopsies of the gastrointestinal tract, skin or salivary glands.[9–16] Moreover, there are first promising findings regarding the identification and characterization of pathological α-syn forms in biofluids, such as the CSF.[17] However, apart from still highly varying outcomes regarding sensitivity and specificity,[13] all these techniques are limited due to their invasiveness. Compared to those options an easy and low-risk obtainable medium is blood plasma or serum.[18] With regard to contaminations and inconsistent α-syn levels in the blood,[18–22] recent studies have focused on extracellular vesicles (EVs).[23–25] EVs released by cells of the CNS (neuron-derived EVs, NEs) have the capacity to pass the blood–brain barrier and transport nucleic acids and proteins including α-syn.[24,26–29] EVs are also thought to contribute to the pathogenesis and development of neurodegenerative diseases by their main functions of intercellular communication and antigen presentation and especially by their capacity to transport and spread neuropathological proteins, e.g. misfolded. α-syn.[30–32] In this paper, the term 'extracellular vesicles' will be used to denote vesicles that are released extracellularly and can be isolated from plasma samples. For a more detailed description of the nomenclature of EVs, please see the article by the International Society for Extracellular Vesicles.[33]

In our study presented here, we describe a methodological approach that combines the isolation and preparation of EVs as well as NEs from blood followed by biochemical characterization of the soluble protein fraction. Using non-denaturing immunoblotting together with a structure-specific antibody detecting pathological α-syn conformers and by applying an adapted α-syn seeding assay, we analysed the structural and functional characteristics of EV/NE-derived α-syn. Both analyses allowed the comparison and discrimination of Parkinson's disease patients from non-Parkinson's disease individuals, indicating the potential of our protocol to reveal a biomarker for Parkinson's disease. Hence, our study provides the proof of concept and basis for the development of a standardized, non-invasive assay that allows the detection of pathology-associated α-syn extracted from blood, reliably discriminating patients from controls.

Materials and methods

Patient samples

Thirty Parkinson's disease patients were recruited from the in- and outpatient clinics of the Department of Neurology at the University Hospital Kiel. Additionally, 50 non-Parkinson's disease individuals were recruited (relatives of patients from the department and patients without any evidence of neuroinflammatory and neurodegenerative disorders). Here, all non-Parkinson's disease individuals are referred as the control group. The inclusion criterion for Parkinson's disease patients was a diagnosis of Parkinson's disease according to the UK Brain Bank Criteria. Exclusion criteria for both groups comprised (i) an inability to perform written performed consent (i.e. Montreal Cognitive Assessment <18 points); and (ii) other diseases affecting the CNS. The study protocol was approved by the local Committee on Ethics and Human Research (D442/2) at the University of Kiel (Germany). Venous blood was collected in heparin tubes (Sarstedt, #04.1936). A total of two full tubes (2 × 7.5 ml) were collected from each patient and each control. Samples were not analysed in a blinded fashion.

Hoehn and Yahr, MDS-UPDRS-III and disease duration

The Hoehn and Yahr score and Movement Disorder Society Unified Parkinson's Disease Rating Scale Part 3 (MDS-UPDRS-III) were used to classify the severity of UPDRS-III on the basis of clinical symptoms. Both were assessed by clinical examination in the Department of Neurology at the University Hospital Kiel at the time of blood collection. The disease duration was indicated in years and calculated from the year of initial diagnosis to the date of blood collection. An overview of Hoehn and Yahr score, MDS-UPDRS-III score, disease duration, age and male gender of both groups can be found in Table 1 and Supplementary Table 1.

Isolation of extracellular vesicles

After the blood samples were collected in heparin tubes, the blood was incubated for 10 min at room temperature. Next, samples were centrifuged at 2500*g* for 10 min at 22°C (Eppendorf Centrifuge,

Table 1 Clinical parameters of analysed cohorts

Category	PD ($n = 30$)	Ctrl ($n = 50$)	P-value
Age, years, mean [range]	67 [46–84]	70 [45–86]	0.66
Male gender, *n* (%)	21 (70)	34 (68)	0.99
Disease duration, years, mean [range]	4 [1–16]	NA	NA
Hoehn and Yahr, points, mean [range]	2 [1–5]	NA	NA
MDS-UPDRS-III, points, mean (SD)	25 (15)	NA	NA

NA = not applicable.

5417R). Supernatants (plasma) were transferred to low binding tubes (Sarstedt, #72.706.600) as 500 µl aliquots and were stored at −80°C. Plasma samples were then centrifuged (2000*g*, 20 min, 22°C) to remove cells and debris. Supernatants containing the partially clarified plasma were transferred to new low binding tubes. Through the next centrifugation step (10 000*g*, 20 min, 22°C) debris were removed. The required volume of clarified plasma (500 µl) was transferred to new tubes, PBS was added in equal parts and samples were mixed using a vortex mixer (MS2 minishaker, IKA). One hundred and fifty microlitres of the EV precipitation reagent (Thermo Fisher, #4484450) was added to each plasma sample (500 µl plasma + 500 µl PBS). After 10 min of incubation at room temperature, samples were centrifuged again (10 000*g*, 5 min, 22°C). Supernatants were discarded and the EV-containing pellets were resuspended. For immunoblotting and seeding assay pellets were resuspended in 30 µl Triton buffer (1% Triton-X100, 10% glycerol, 150 mM NaCl, 25 mM HEPES at pH 7.4, 1 mM EDTA, 1.5 mM $MgCl_2$) containing 1× protease inhibitor cocktail (cOmplete Protease Inhibitor Cocktail, Roche, #11836145001), 50 mM NaF, 2 mM $NaVO_4$ and 1 mM phenylmethylsulphonyl fluoride (PMSF). For transmission electron microscopy (TEM) imaging and dynamic light scattering (DLS) measurements pellets were resuspended in 50 µl NaCl (0.9%). For immunoblot analyses, samples were incubated for 30 min on ice. After centrifugation for 5 min at 4°C for 2100*g* supernatants were centrifuged through ultracentrifugation at 100 000*g* for 30 min at 4°C (Beckman OptimaTM TLX Ultracentrifuge, Instrument-Typ CO-TLX 120). Supernatants (Triton-soluble fractions) were used for further analyses. Protein concentrations were measured by bicinchoninic acid (BCA) assay (Pierce, #23227).

Purification of neuron-derived EVs

EVs purified from 500 µl of blood plasma (see above) were resuspended in 300 µl of PBS and incubated at 4°C rotation overnight with 2 µg of anti-neuronal cell adhesion molecule L1 (NCAM-L1) antibody (Santa Cruz, #sc-514360). For each sample, 30 µl beads (Protein A/G PLUS-Agarose, Santa Cruz, #sc-2003, lot no. J0920) were blocked in 2% bovine serum albumin and incubated at 4°C rotation overnight. The next day, blocked beads were washed three times using mild lysis buffer (40 mM HEPES, pH 7.4, 120 mM NaCl, 1 mM EDTA, 0.3% CHAPS, 10% glycerol). After the last washing step 30 µl of mild lysis buffer were added for each sample to the beads and subsequently 30 µl of these washed and blocked beads were added to each EV resuspension with antibodies for 4 h at 4°C with rotation. After collecting the immunoprecipitates by centrifugation (1000*g*, 5 min, 4°C), supernatants were discarded. Pellets were washed using mild lysis buffer. Following the last centrifugation step pellets were resuspended in Triton buffer (1% Triton-X100, 10% glycerol, 150 mM NaCl, 25 mM HEPES at pH 7.4, 1 mM EDTA, 1.5 mM $MgCl_2$) containing 1× protease inhibitor cocktail (cOmplete Protease Inhibitor Cocktail, Roche, #11836145001), 50 mM NaF, 2 mM $NaVO_4$ and 1 mM PMSF. Samples were incubated for 30 min on ice before subjection to ultracentrifugation for sequential protein extraction [100 000*g*, 30 min, 4°C (Beckman Optima™ TLX Ultracentrifuge, Instrument-Typ CO-TLX 120)]. Supernatants (Triton-soluble fractions) were used for further analyses using an immunoblotting and seeding assay. For TEM imaging/DLS measurements pellets were resuspended in 50 µl of NaCl (0.9%). Protein concentrations were measured by BCA (Pierce, #23227). For the following analyses NEs of 4 ml of plasma of each single Parkinson's disease patient and control were merged, for α-syn detection in western blot analyses NEs of 8 ml of plasma were merged. To approximate the NE proportion of the total of EVs, we calculated the percentage of NE concentration to the EV concentration for each patient and control, which revealed a range of 2–6%.

Lysis of samples and native dot blot analysis

After sequential protein extraction using ultracentrifugation as described previously and in Zunke *et al.*[34] (100 000*g*, 30 min, 4°C, Beckman Optima™ TLX Ultracentrifuge, Instrument-Typ CO-TLX 120), Triton-soluble fractions of EVs and NEs were used for BCA protein assay. Plasma samples were used for BCA protein assay after removing debris and cells by the first two centrifugation steps described previously without any further treatments. Plasma samples, soluble fractions of EVs and NEs were subjected to immunoblot analyses (dot blot/western blot). For dot blot analyses 7.5 µg/10 µg of total protein were applied in 2.5-µL dots onto nitrocellulose membranes (#10600001, Amersham Biosciences), air-dried for 5 h and blocked in Tris-buffered saline (TBS) with 5% (w/v) non-fat dry milk for 1 h. Primary antibodies (Supplementary Table 2) were incubated overnight in TBS-Tween (1%) containing 5% non-fat dry milk. Secondary fluorescent-conjugated antibodies (Supplementary Table 2) were incubated for 1 h after washing the membranes with TBS-Tween (1%). Detection and digitalization were carried out using the Amersham Typhoon Biomolecular Imager (GE Lifesciences). Samples were dot blotted under native conditions for structure-specific readouts. As loading control total protein staining was used (Direct Blue 71, Sigma-Aldrich, #212407). Antibody signal intensities were normalized to loading control (total protein).

SDS–PAGE, western blot analysis and silver staining

For sodium dodecyl sulphate–polyacrylamide gel electrophoresis (SDS–PAGE) analyses, samples were boiled in Laemmli buffer (5× stock: 250 mM Tris/HCl, pH 6.8, 10% SDS, 50% glycerol, 0.5% bromphenol blue and freshly added 5% 2-mercaptoethanol). The total volume of each sample (~10/20 µl, 10/20/40 µg) was loaded on 10 or 12% Tris-glycine gel and subjected for a duration of 1.5–2 h to electrophoresis using Thermo Fisher Scientific electrophoresis chambers (Mini gel tank, #A25977). Proteins were transferred to polyvinylidene difluoride membranes (Merck Millipore, #IPFL00010). Membranes were fixed with 0.4% paraformaldehyde in PBS for 20 min and blocked in TBS (1%) with 5% (w/v) non-fat dry milk for 1 h. Primary antibodies (Supplementary Table 2) were incubated overnight at 4°C and detection was performed after using secondary fluorescent-conjugated antibodies (Supplementary Table 2) for 1 h at room temperature. Detection was carried out by the Amersham Typhoon Biomolecular Imager (GE Lifesciences). Coomassie staining of the gels (incubation in 0.02% Coomassie Brilliant Blue G-250 Dye [Thermo Scientific™, #20272), 10% ethanol (96%), 2% orthophosphoric acid (100%), 5% aluminiumsulphat-(14-18)-hydrat] was used as a loading control.

Silver staining of SDS gels was performed as described in the manufacturer's protocol (Pierce, #24612).

Preparation of recombinant α-synuclein

Human recombinant monomeric α-syn was used and prepared as previously described.[35] In brief, by bacterial transformation of the human α-syn PT7-7 construct (a gift from Dr Hilal Lashuel, Addgene plasmid #36046; RRID: Addgene_36046[36]) human α-syn was expressed in *E. coli* BL21 (DE3) pLysS competent cells (Novagen). Next, recombinant α-syn was isolated from *E. coli* by several purification steps, which included boiling and ion exchange chromatography [Resource-Q 6 ml column (GE Healthcare)]. Subsequently, monomeric α-syn was purified by size-exclusion chromatography using a SuperdexTM 75 10/300 column (GE Healthcare). The preparation of α-syn aggregates—such as fibrils—was carried out by agitation (1000 rpm) of monomeric α-syn in a concentration of 3.4 µg/µl with a 3 mm polytetrafluoroethylene bead (Polyscience) in a Tris/HCl buffer (0.1 M, pH 7.4). Successful fibril formation was validated by measurement of Thioflavin T (ThT) fluorescence.

α-Synuclein seeding assay

α-Syn seeding assay was performed by further adjusting a published protocol[37] and is explained in detail next. To amplify pathological α-syn conformers derived from plasma/EVs/NEs, 10 µg of total protein of control and Parkinson's disease samples were incubated with 100 ng of recombinant monomeric α-syn in a total volume of 100 µl of PBS in a dark 96-well plate (Thermo Fisher Scientific, #237108). After covering the plates with silicon lids (Thermo Fisher Scientific, #AB0566) and PARAFILM® M sealing film (Bemis) they were incubated at 37°C and agitated at 1000 rpm using a plate shaker (MTS 4, IKA), then placed in the incubator. Before each measurement, 1 µl of ThT [1 mM stock solution (end concentration of 0.01 mM) freshly prepared before each measurement] was manually added to each well, indicating an increasing ThT content after each measurement. After a single measurement, the plates were replaced on the plate shaker in the incubator. ThT fluorescence was monitored over time at the indicated time points and measured at an excitation of 410 nm and emission of 475 nm using a microplate reader (Infinite® 200 PRO, Tecan). Measurements were stopped when ThT fluorescence plateaued. Measurement time points were chosen corresponding to the course of the positive control curve. For structural [TEM, circular dichroism (CD) spectroscopy, silver staining] and dot blot analyses, we performed in parallel the seeding assay under the same conditions without addition of ThT. In this study, several seeding rounds were performed to demonstrate the effect of pathological α-syn on monomeric recombinant α-syn. For subsequent rounds of seeding assay, 10 µl of the amplified end product of the previous round were added to 100 ng of recombinant α-syn in a total volume of 100 µl of PBS and subjected to agitation as described previously. Pre-formed α-syn fibrils (10 µl of 0.68 ng/µl) and the presence of 100 ng of α-syn monomers were used as positive controls. As negative controls, 100 ng α-syn monomers (without further seed) as well as only pre-formed fibrils (10 µl of 0.68 ng/µl; without monomeric α-syn) were used. Analyses show total ThT signals in arbitrary units.

Transmission electron microscopy of vesicles and seeding assay end products

Negative-stain TEM was performed as previously described.[38] After isolation of EVs as well as NEs, the vesicle-containing pellets were resuspended in 0.9% NaCl. Further, buffer exchanging was performed as described in the manufacturer's protocol of Zeba™ Spin Desalting Columns (Thermo Fisher, #89882). Isolated and buffer exchanged (100 mM Tris-HCl, pH 6.8) samples containing EVs or NEs were diluted to the final concentration of 0.5 µg/µl and 3 µl were added on a previously glow discharged (25 mA, 30 s) carbon-coated electron microscopy (EM) grid (Electron Microscopy Sciences) followed by incubation on an EM grid for 30 s. Seeding assay end products were used without dilution. Subsequently, the sample solution was removed using filter paper and the EM grid was contrasted twice with 1% aqueous uranyl acetate solution (Merck Millipore). The excess of the stain solution was removed with filter paper and the EM grid was air-dried. After transfer of the grid into a JEOL 1400 Plus TEM (JEOL) operating at 100 kV, images were taken at a magnification of ×30.000 to ×50.000. Size measurements were performed by utilizing ImageJ software (FIJI, v.2.0.0).

Dynamic light scattering

EVs/NEs were isolated as described before and each sample was adjusted to 1 µg/µl protein concentration. Measurements were performed as described before.[39] Briefly, samples were prepared in triplicate, added in to precision cells (Quartz SUPRASIL®, Hellma) and measured 10 times with a 90° scattering angle at 20°C using the Spectroscatter 201 (RiNA GmbH).

Circular dichroism spectroscopy

Samples derived from the sixth round of seeding assay were subjected to CD measurements after the end of seeding assay (plateau phase). Samples were measured at room temperature using a JASCO J-720 CD spectropolarimeter (JASCO) with 0.5 nm pathlength cuvettes (using ~80 µl/sample). Spectra were recorded from 190–250 nm wavelengths.

Schematic illustration

The illustrations in Figs 1A and 2A and the thumbnail were created using Smart Servier Medical Art (http://smart.servier.com/), which is licensed under CC BY 3.0.

Quantification and statistical analyses

Statistical analyses of clinical parameters were performed using SPSS 26.0 (SPSS Inc., IBM, USA) and variables were tested for statistical distribution using the Kolmogorov–Smirnov test. Group comparisons were performed with the Fisher's exact test and the Mann–Whitney *U*-test or *t*-test. Signal intensities of immunoblot analyses were quantified by using ImageJ software (FIJI, v.2.0.0) using background subtraction. Regions of interest were drawn around the dots and integrated density was measured. Antibody signals were normalized to total protein level as loading control. Analyses and data management was done using Prism 7 (GraphPad Software, v.7.0a) and Excel (Microsoft, v.15.33). Statistical analyses were performed and graphs created using Prism 7 (GraphPad Software, v.7.0a). Data-points and column data are depicted as mean ± SEM as described in corresponding figure legends. An unpaired two-tailed Student's *t*-test was used for pairwise comparison, two-way ANOVA with Tukey or Sidak's multiple comparison tests were used for group comparisons. For statistical analyses, a Gaussian distribution was assumed. Data are shown as mean and statistical significance was obtained when $^{*}P < 0.05$, $^{**}P < 0.01$, $^{***}P < 0.001$ and $^{****}P < 0.0001$. Individual *P*-values as well as *n* numbers are mentioned in corresponding figures.

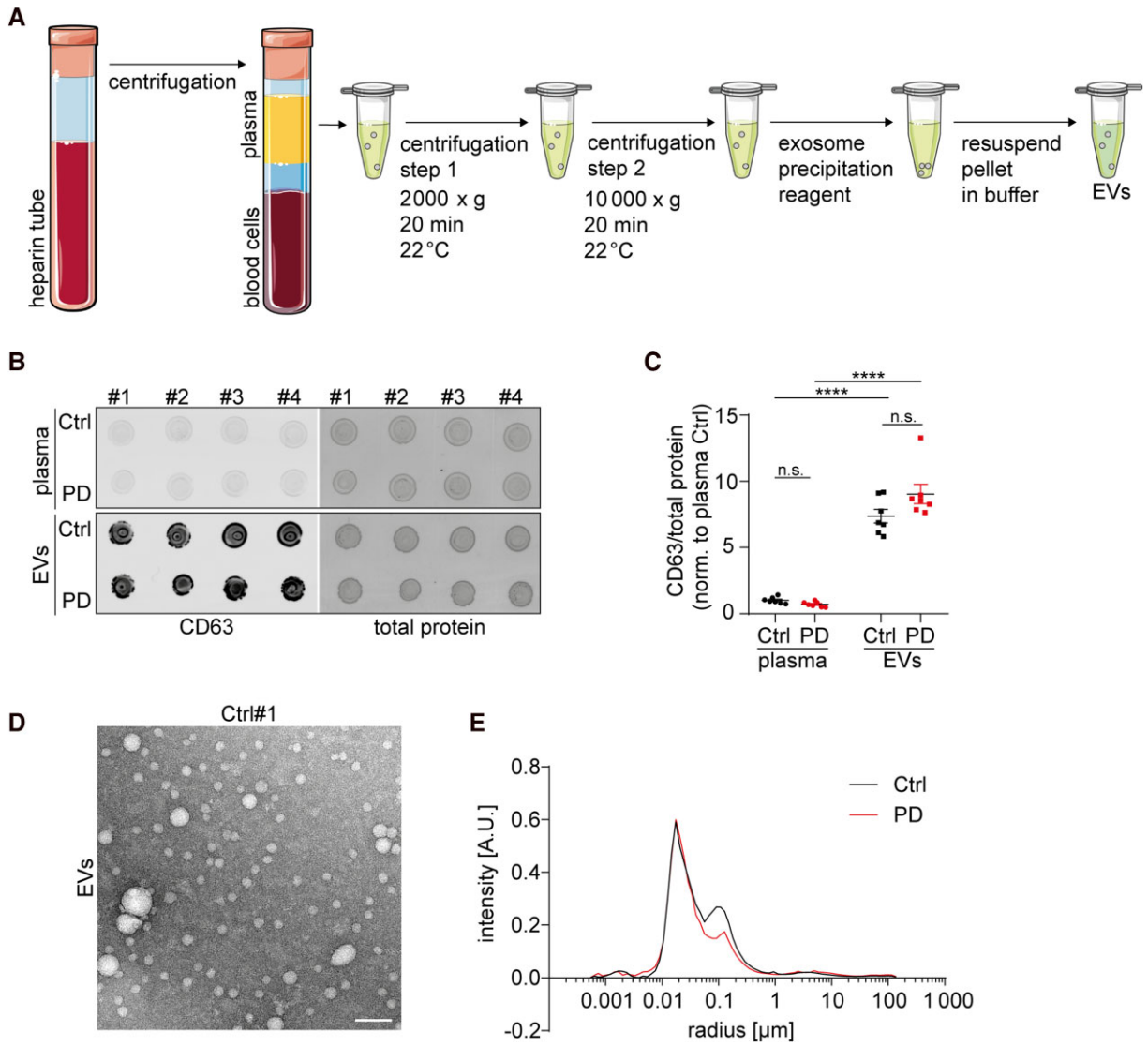

Figure 1 Isolation and characterization of plasma-derived EVs. (**A**) Schematic illustration of used protocol to isolate EVs from human plasma samples. Blood of Parkinson's disease patients and controls was collected. After several centrifugation steps and treatment with the EV precipitation reagent, EVs were purified. (**B**) Representative dot blot analysis of plasma samples and plasma-derived EVs. Samples were dot blotted under native conditions and stained with anti-CD63 antibody. As loading control total protein was used. (**C**) Quantification of CD63 signal intensity normalized to total protein. Each data-point represents one individual Parkinson's disease patient or control individual ($n = 7$). (**D**) Representative transmission electron micrograph from EVs of a control individual. Scale bar = 100 nm. Images of analysed samples and related size distribution measurements can be found in Supplementary Fig. 1D ($n = 3$). (**E**) Representative DLS measurement of particle size distribution of plasma-EVs from Parkinson's disease patients and controls ($n = 3$). Statistical analyses were performed using two-way ANOVA with Tukey multiple comparison test. Data are shown as mean ± SEM and statistical significance was specified in terms of n.s. being not significant and ****$P < 0.0001$.

Data availability

All raw data, raw values for all analyses (e.g. dot blots) and endpoints of measurements of performed α-syn seeding assays as well as further additional information are available on request.

Results

Demographics

Plasma samples were collected from 30 patients with Parkinson's disease (mean age 67 years, range 46–84 years) and 50 controls (mean age 70 years, range 45–86 years). There was no age distribution difference among the groups ($P = 0.66$). Mean disease duration of Parkinson's disease patients was 4 (1–16) years and mean clinical motor symptom score (MDS-UPDRS-III) was 25. Summarized data of both groups are listed in Table 1; available clinical data for each patient/control is listed in the Supplementary Table 1. Subsequent biochemical analyses were performed in a non-blinded fashion. In all figures and tables, we use the abbreviated terms 'PD' for Parkinson's disease patients and 'Ctrl' for control individuals that do not exhibit Parkinson disease pathologies or any other neurodegenerative disorders.

Isolation and detection of extracellular vesicles from peripheral blood

After gradual centrifugation and EV precipitation (Fig. 1A), the isolation of EVs was confirmed through immunoblotting, DLS and TEM.

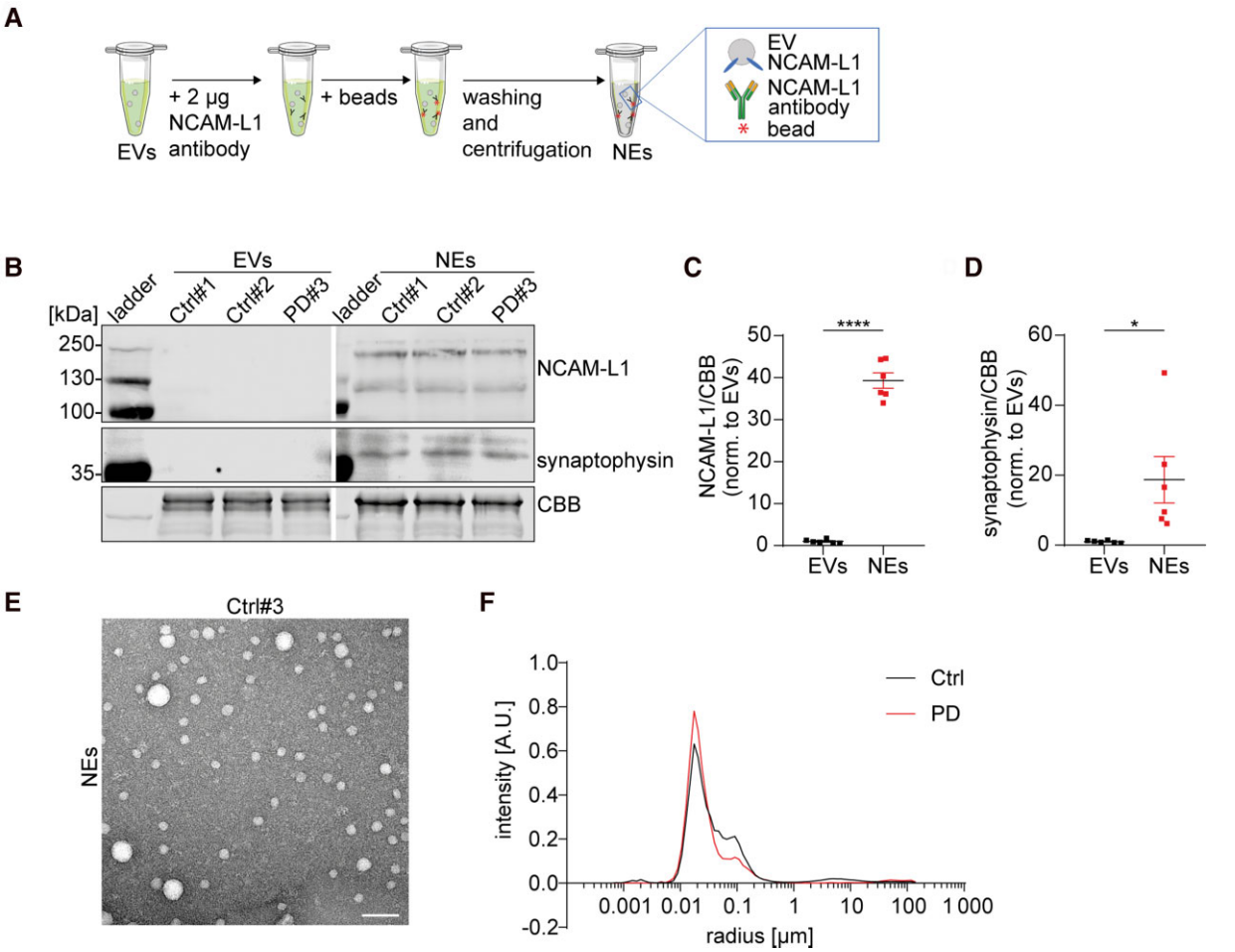

Figure 2 Isolation of NEs and comparison to EVs. (**A**) Schematic figure of the isolation of NEs using an immune-affinity capturing protocol. Vesicles containing NCAM-L1 were precipitated. (**B**) Representative western blot analysis of EV- and NE-containing samples. As neuronal markers, anti-NCAM-L1 (~220, ~120 kDa) and anti-synaptophysin (~38 kDa) antibodies were used for the detection of NEs. Coomassie Brilliant Blue (CBB) was used as loading control. Gap indicates separation of the same blot. (**C** and **D**) Quantification of NCAM-L1 and synaptophysin after normalization to CBB ($n = 6$). Data-points represent single Parkinson's disease or control individuals. (**E**) Representative transmission electron micrograph of purified NEs. Scale bar = 100 nm. Images of analysed samples and related size distribution measurements can be found in Supplementary Fig. 2I ($n = 3$). (**F**) DLS measurement of particle size distribution of NEs from Parkinson's disease patients and controls ($n = 3$). Data are shown as mean ± SEM and statistical significance was determined by unpaired two-tailed Student's *t*-test. $^{*}P < 0.05$ and $^{****}P < 0.0001$.

Enrichment of EVs was further evaluated through dot blot and western blot analyses in comparison to native plasma samples (Fig. 1B and Supplementary Fig. 1A). In both analyses, the EV marker CD63 was significantly enriched in the EV fraction after normalization to total protein (Fig. 1B and C and Supplementary Fig. 1A). Moreover, no difference in CD63 signal could be observed between Parkinson's disease and control samples (Supplementary Fig. 1B and C). Enhanced CD63 levels within the fraction of EVs indicated a sufficient protocol for enrichment of EVs. Further characterization of the size and morphology of EVs was gained by negative-stain TEM as well as DLS and showed a homogenous preparation of EVs (TEM: Fig. 1D and Supplementary Fig. 1D and E; DLS: Fig. 1E). Both analyses confirmed the presence of uniform particles that corresponded to the size of EVs as described in literature.[23] Moreover, analysed samples of Parkinson's disease patients and controls exhibited no differences in mean radius distribution according to the TEM- and DLS-based size distribution (TEM: Supplementary Fig. 1E; DLS: Fig. 1E). As an assay control, a TEM image of the exosome precipitation reagent is shown in Supplementary Fig. 1F. In summary, we demonstrate the efficient EV-isolation from blood plasma, exhibiting no differences in size or morphology between patients and controls. Demonstration of isolation and detection of EVs from peripheral blood was performed as basis for further analyses in a subset of 15 patients and 15 controls (Fig. 1 and Supplementary Fig. 1).

Identification of neuron-derived extracellular vesicles from peripheral blood

The purification of NEs through immunoprecipitation (Fig. 2A) revealed significantly increased signals of the different isoforms of the neuronal cell adhesion molecule L1 (NCAM-L1) when compared to plasma-derived EVs using western blot analysis (Fig. 2B and C and Supplementary Fig. 2A). Thereby, unspecific binding to the anti-NCAM-L1 antibody and non-specific signals by the anti-NCAM-L1 antibody with beads could be excluded through western blot analysis (Supplementary Fig. 2D). For both, EVs as well as NEs, commonly used EV markers such as CD63, CD9 or

CD81 showed strong signals using immunoblot analyses (Supplementary Fig. 2A–C, E and F). In comparison to EVs, immunoblot analyses of NEs further revealed a significant increase in neuronal markers: synaptophysin (Fig. 2B and D)[40] and neuron-specific enolase (Supplementary Fig. 2E and G).[41,42] This confirmed the homogenous and neuronal origin of precipitated NEs. Importantly, α-syn was detected by western blot analyses within the fraction of NEs (Supplementary Fig. 2E and H). Additionally, TEM and DLS analyses of Parkinson's disease patient-NEs and control NEs showed similar size distributions indicating uniform characteristics (size and morphology) of isolated NEs (TEM: Fig. 2E and Supplementary Fig. 2I and J; DLS: Fig. 2F). As an assay control, a TEM image of the beads only is shown in Supplementary Fig. 2K. Further, TEM and DLS studies of NEs revealed no significant differences between Parkinson's disease patients and controls. All results shown in Fig. 2 and Supplementary Fig. 2 were performed in a subset of 15 patients and 15 controls as the basis for further analyses.

Detection of α-synuclein within soluble fraction of neuron-derived extracellular vesicles

α-Syn signals were visualized through western blotting of the Triton-soluble fraction of isolated NEs (Fig. 3A). Using a C-terminal α-syn antibody (C-20) and denaturing conditions, all tested samples showed similar α-syn signal intensities without significant differences in signal intensity between Parkinson's disease patients and controls (Fig. 3A and B and Supplementary Fig. 3A). Next to α-syn, signal intensities of neuronal markers like NCAM-L1, synaptophysin or the pan-neuronal marker protein gene product 9.5 showed also no differences between patients and controls (Supplementary Fig. 3A–D). The presence of pathological α-syn forms was analysed through the structure-specific α-syn antibody MJFR-14-6-4-2 (MJFR) (Fig. 3C) that was raised against pathological α-syn conformers comprising fibrillary structures.[43] To preserve structure-specific epitopes, dot blot analyses were performed with samples that were not exposed to reducing or denaturing reagents and conditions. The antibody specificity was validated and exhibited concentration-dependent binding to *in vitro* produced α-syn filaments and showed negligible interaction with recombinant monomeric α-syn using 5 ng of protein in dot blot analysis (Supplementary Fig. 3E–G). In addition, unspecific signal and binding of the secondary antibody was excluded (Supplementary Fig. 3H). Interestingly, using non-denaturing conditions and the structure-specific α-syn antibody (MJFR), NEs from Parkinson's disease patients exhibited significantly increased signal intensities in comparison to control NEs (Fig. 3D and E). This difference only persisted within the native, Triton-soluble fraction of NE lysates derived after ultracentrifugation (Supplementary Fig. 3I). Applying another structure-specific antibody recognizing a generic epitope common to amyloid protein structures (OC) also exhibited significantly higher signal intensities in NEs of Parkinson's disease patients in comparison to control NEs (Fig. 3F and G). Using the Syn-1 antibody (not confirmation specific), no significant difference in the signal intensities between Parkinson's disease and control samples was detected (Fig. 3H and I). Taken together, quantitative analysis of total α-syn in NEs showed no significant differences between Parkinson's disease patients and controls. However, only the application of pathology-associated antibodies and native sample conditions exhibited increased antibody signals of Parkinson's disease patient-NEs comparing Ctrl-NEs.

Amplification of α-synuclein from neurin-derived extracellular vesicles

The capacity of NE-derived α-syn to seed pathological amyloid protein aggregation was tested using a seeding assay optimized for α-syn,[37,44,45] which we modified for our purposes (see 'Materials and methods' section). For this approach, samples (plasma, soluble lysates of EVs and NEs) were incubated with recombinant monomeric α-syn and agitated at 37°C over time. The amyloid protein formation was monitored by an increase in ThT fluorescence, indicating amyloid protein folding, until fluorescence signals plateaued. ThT fluorescence of recombinant, pre-formed α-syn fibrils (input: 10 µl 0.68 ng/µl, 100 ng monomeric α-syn) was used as positive control, α-syn monomers (without seed) and α-syn fibrils (without α-syn monomers) were used as negative controls (Supplementary Fig. 4A). All analyses in Fig. 4 show samples subjected to six rounds of protein amplification.

α-Syn seeding assay analyses of native plasma samples of Parkinson's disease and control individuals showed no increase in ThT signals over time (Fig. 4A and Supplementary Fig. 4B). In addition, we analysed the signal intensity after incubation with the MJFR antibody of the untreated plasma samples after seeding assay by dot blot analysis indicating no significant difference between Parkinson's disease and control plasma (Fig. 4B and C and Supplementary Fig. 4H and I). Seeding assay analysis of plasma-isolated EVs is shown in Fig. 4D (Supplementary Fig. 4C). After 20 h of incubation ThT signals of Parkinson's disease patient-EVs started to increase significantly in comparison to the EVs of control individuals. After 30 h, ThT fluorescence signals plateaued until the end of the experiment. Corresponding dot blot analysis indicated significant differences in MJFR intensity comparing Parkinson's disease patient-EVs and control-EVs after six rounds of seeding assay (Fig. 4E and F and Supplementary Fig. 4J and K). Interestingly, there was no significant difference in MJFR signal intensities between the Parkinson's disease and the control group before amplification of EV-derived α-syn via seeding assay (Supplementary Fig. 4J and K). α-Syn seeding assay analyses of soluble lysates of NEs derived from Parkinson's disease patients and controls are shown in Fig. 4G. At 20 h of incubation, ThT signal intensities were significantly increased in samples of Parkinson's disease patients in comparison to samples from control individuals (Fig. 4G). After 30 h, ThT fluorescence plateaued and was stable until the end of the experiment. Dot blot analyses of amplified samples, applying the structure-specific MJFR antibody, showed no overlap of signal intensities between Parkinson's disease patients and control individuals, so both groups could be clearly separated by their α-syn signal (Fig. 4H and I and Supplementary Fig. 4L and M). As shown in Fig. 3D and E and Supplementary Fig. 4L and M, significant differences in MJFR signal between Parkinson's disease patient-NEs and control-NEs were already observed in dot blot analyses before using the seeding assay. Supplementary Fig. 4G shows increasing ThT signal intensities from each amplification round (round one-five) using NE samples as well as recombinant α-syn protein as control, suggesting step-wise enrichment of amyloid α-syn conformers. All individual ThT signal curves of all analysed NE-containing samples of Parkinson's disease patients ($n = 30$) and controls ($n = 50$) subjected to the sixth seeding assay round are depicted in Supplementary Fig. 4D–F.

To exclude potential contamination by erythrocytes/haemoglobin, we analysed levels of haemoglobin ß via dot blotting before and after performance of the seeding assay of the respective lysates (plasma/EVs/NEs) (Supplementary Fig. 4H–M).

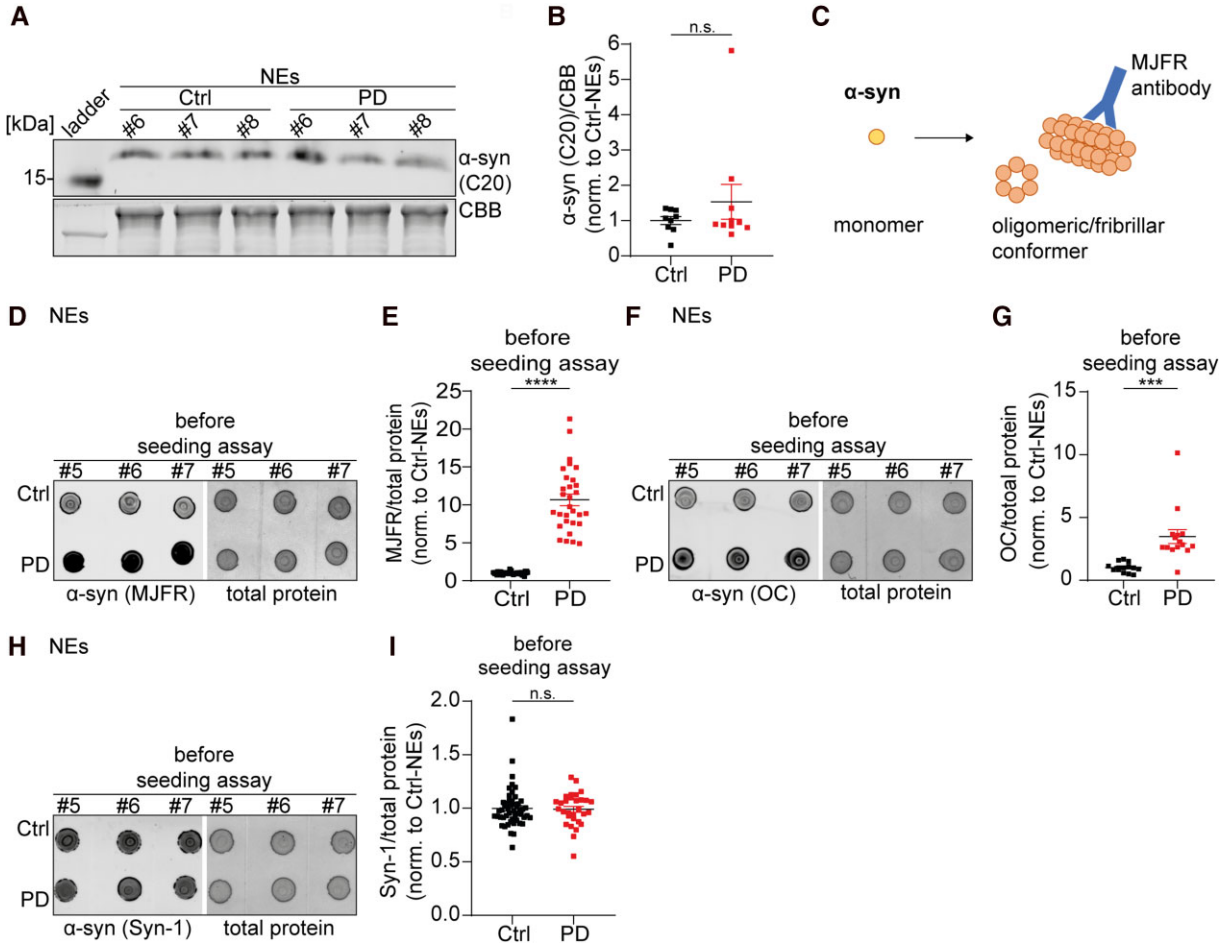

Figure 3 Detection of different α-syn forms within NEs. (**A**) Representative immunoblot of NE-containing samples of Parkinson's disease and control individuals using an anti-α-syn antibody (C20). Coomassie Brilliant Blue (CBB) was used as loading control. (**B**) Quantitative analysis of C20 antibody signal intensity normalized to Coomassie Brilliant Blue. Each data-point represents one Parkinson's disease ($n = 10$) or control ($n = 9$) individual. (**C**) Schematic demonstration of the different structural conformations of α-syn. In its native form, α-syn presents as soluble monomer or physiological oligomer. Under pathological conditions, α-syn oligomerization/fibrillization is triggered and this conformation is detected by the MJFR antibody. In our study, we focus on the detection of this pathological α-syn species. (**D**) Representative dot blot of Parkinson's disease patient-NEs and control NEs after staining with the MJFR antibody. Total protein was used as loading control. (**E**) Respective densitometry of MJFR antibody signal intensities of analysed Parkinson's disease ($n = 30$) and control ($n = 50$) subjects. (**F**) Representative dot blot of Parkinson's disease patient-NEs and control NEs using the OC antibody that detects amyloid protein folding. (**G**) Quantification of OC antibody signal intensities. Each sample is shown as single data-point ($n = 15$). (**H**) Representative dot blot of Parkinson's disease patient-NEs and control NEs using the Syn-1 antibody (not confirmation specific). (**I**) Respective densitometry of Syn-1 antibody signal intensities of analysed Parkinson's disease ($n = 30$) and control ($n = 50$) individuals. Further dot blots of NE samples and their analyses are shown in Supplementary Fig. 4L and M. Data are shown as mean ± SEM and statistical significance was determined by unpaired two-tailed Student's t-test. n.s. = not significant; $^{***}P < 0.001$ and $^{****}P < 0.0001$.

Structural characterization of amplified neuronal α-synuclein

Pathological α-syn forms derived from soluble lysates of NEs and amplified by α-syn seeding assay (six rounds) were further characterized by biochemical and biophysical analyses. CD spectroscopy of α-syn conformers exhibited a minimum extension around 220 nm indicating the presence of predominantly β-sheet rich structures in samples derived from Parkinson's disease patients (Fig. 5A). In contrast, spectra of analysed control samples did not exhibit β-sheet characteristics (Fig. 5A). Spectra of all analysed Parkinson's disease patients and controls are shown in Supplementary Fig. 5A. Next, amplified α-syn was visualized through silver staining after denaturing SDS–PAGE (Supplementary Fig. 5B). For this purpose, seeding assay end products of NEs were centrifuged (sedimented), and the resulting pellets were resuspended and subjected to electrophoresis before silver staining followed. For all analysed Parkinson's disease samples, this resulted in a protein band at ~16 kDa, corresponding to the size of monomeric α-syn (Supplementary Fig. 5B).[17,34,37] For ultrastructural analyses, end products of the α-syn seeding assay were analysed by TEM, indicating oligomeric and fibrillary structures of α-syn derived from Parkinson's disease patient-NEs (Fig. 5B and Supplementary Fig. 5C). α-Syn conformers with complex structures were absent after seeding assay of control-NEs (Supplementary Fig. 5D). Altogether, our data demonstrate the ability of soluble α-syn conformers derived from Parkinson's disease patient-NEs to seed amyloid protein aggregation. Biochemical and biophysical as well as morphological analyses revealed that this amplified NE-derived α-syn species formed aggregates exhibiting β-sheet rich conformations and are organized into fibrillary structures.

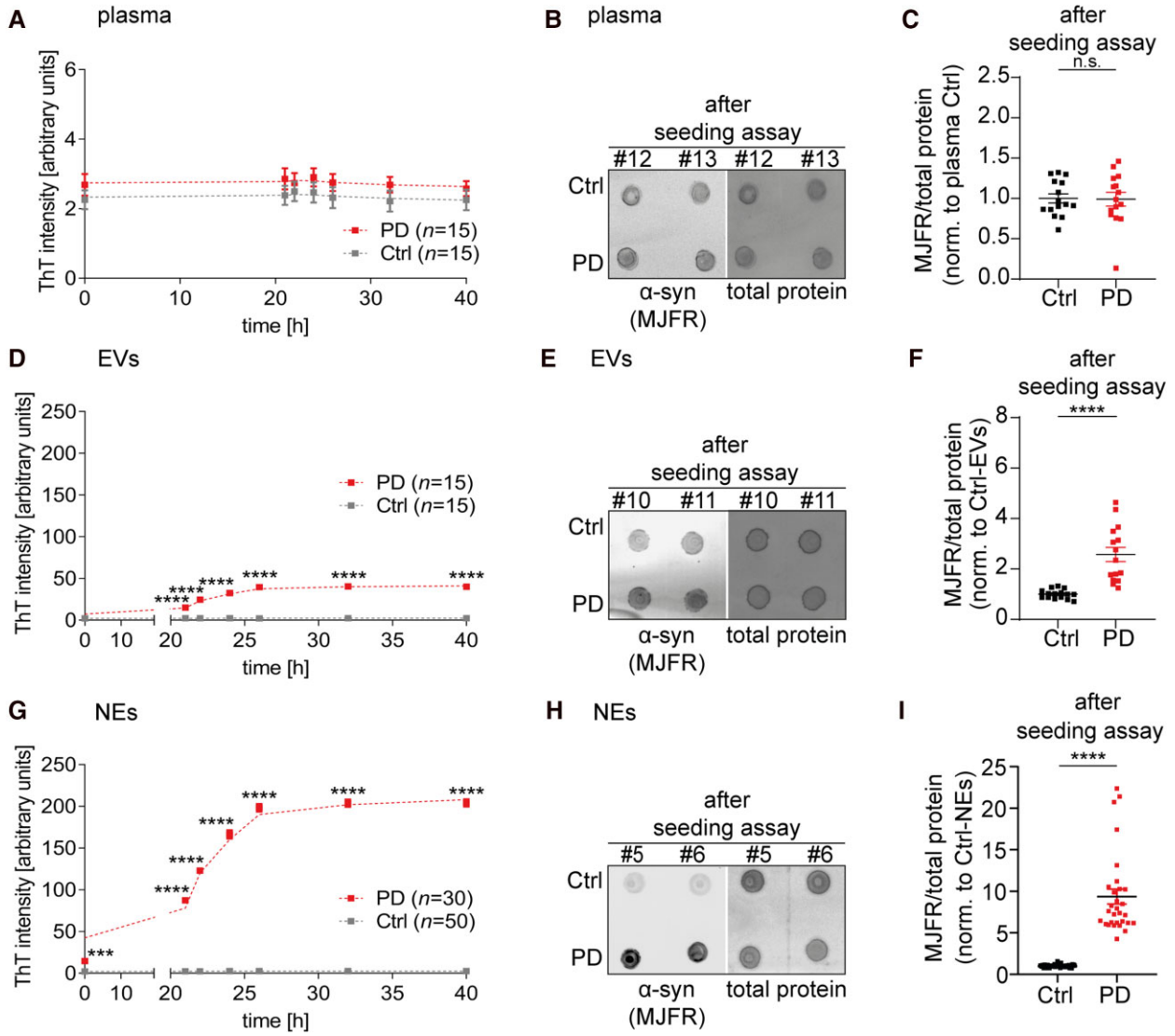

Figure 4 Amplification of α-syn derived from NEs. (**A**) Total ThT signal intensity over time during the sixth round of seeding assay using plasma samples derived from Parkinson's disease patients and control subjects ($n = 15$). Data are shown as smoothed curves of total ThT signals (mean ± SEM) of combined individual measurements of 15 Parkinson's disease and 15 control samples for each time point. (**B**) Representative dot blot of plasma samples of Parkinson's disease and control subjects after six rounds of seeding assay using the MJFR antibody. Total protein was used as loading control. (**C**) Respective densitometry of MJFR antibody signal intensities of all 15 analysed Parkinson's disease and 15 control samples after normalization to total protein. (**D**) Total ThT signals over time during the sixth round of seeding assay of plasma-derived EVs from Parkinson's disease patients and controls ($n = 15$). (**E**) Representative immunoblot of EVs of Parkinson's disease and control subjects after the sixth round of seeding assay using the MJFR antibody. Total protein was used as the loading control. (**F**) Quantification of MJFR antibody signal intensities of the analysed Parkinson's disease and control individuals after normalization to total protein ($n = 15$). (**G**) Total ThT signal intensity of Parkinson's disease patient-NEs and control-NEs is shown as smoothed curves over 40 h during the sixth round of seeding assay. For each time point, measurements of all 30 Parkinson's disease patients and all 50 controls were combined and demonstrated as means ± SEM. For Parkinson's disease samples a sigmoidal increase in ThT signal is shown, whereas no increase in ThT signal for control samples could be observed. (**H**) Representative dot blot of Parkinson's disease patient-NEs and control-NEs after the sixth round of seeding assay and staining with the MJFR antibody. (**I**) Analyses of MJFR antibody signal intensities normalized to total protein after seeding assay (30 Parkinson's disease patients, 50 controls). For statistical analyses, unpaired two-tailed Student's *t*-test and two-way ANOVA with Sidak's multiple comparison test were applied with n.s. being not significant and ****$P < 0.0001$. Supplementary Fig. 4B–F show an overview of individual datasets of the sixth seeding assay round ThT signal curves; Supplementary Fig. 4H–M show an overview of further representative dot blot analyses.

Discussion

The results of our study clearly demonstrate that a pathological soluble α-syn form can be extracted and amplified from NEs derived from the blood plasma of Parkinson's disease patients. The biochemical and biophysical characterization of the amplified α-syn conformers defined β-sheet and amyloid rich characteristics. The underlying pathological α-syn conformer was detected in all Parkinson's disease patients ($n = 30$) without any exception and clearly distinguished Parkinson's disease samples from the control group ($n = 50$) and vice versa. Moreover, we show the *in vitro* seeding capacity of the NE-associated CNS-derived α-syn forms, which is known to be specific for pathological α-syn conformation.[37,44,45] We conclude that the detection and amplification of pathological,

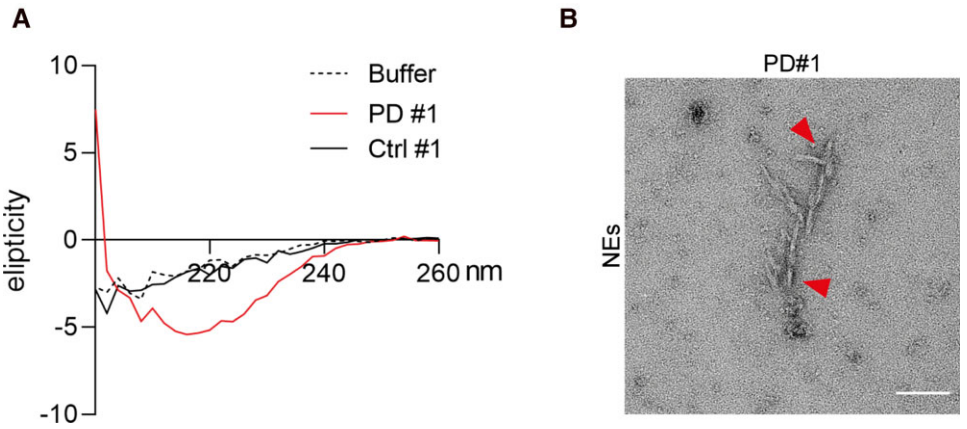

Figure 5 Structural characterization of seeding assay end products. (**A**) Representative CD spectroscopy of formed α-syn aggregates derived from the sixth round of seeding assay. Amplified Parkinson's disease patient-NE-derived α-syn species exhibit β-sheet rich structures as indicated by a minimum extension at around 210–220 nm. Control sample subjected to six rounds of seeding assay shows spectra of the unfolded α-syn. All single spectra of analysed samples are shown in Supplementary Fig. 5A ($n = 3$). (**B**) Representative TEM image of amplified Parkinson's disease patient-NE-derived α-syn conformers after six rounds of seeding assay. Arrowheads indicate fibrillary protein conformations. Scale bar = 100 nm. Representative TEM image of control NEs seeding assay end product of the sixth round can be found in Supplementary Fig. 5D.

soluble α-syn conformers in plasma-NEs is highly promising as a reliable pre-mortem biomarker for Parkinson's disease.

Regarding the urgent need for a biomarker of Parkinson's disease, the detection of α-syn in biofluids has been at the centre of attention in recent years. Several reports demonstrated mostly consistent findings regarding the detection of α-syn in CSF (lower α-syn concentrations in patients with Parkinson's disease), but the invasive nature of lumbar punctures limit the clinical practicability in the routine.[16,46–48] Moreover, further limitations such as large variations in CSF total α-syn values between studies and falsely increased values by blood contaminations must be considered.[48,49] Hence, several meta-analyses of peripheral tissues showed limited sensitivity and specificity.[13,16,50,51] Equally, several studies analysing α-syn levels in blood serum or plasma showed inconsistent findings and the risk of erythrocyte contamination or measurement of intra-erythrocyte α-syn species.[19,21,24,48,52]

Importantly, recent literature provides evidence that CNS-derived α-syn is able to enter the blood stream within EVs.[24,26] The origin of the EV-subspecies is defined within the endosomal network.[53] Briefly, they are formed by inward budding of membranes of multi-vesicular bodies, which release exosomes by fusing with the plasma membrane.[53] EVs are released by most cell types and may carry unique, disease-specific cargo.[24,53–55] One of the key characteristics of EVs is their ability to pass the blood–brain barrier and travel between CNS and peripheral circulation.[27,28] Some of their functions such as cell-to-cell communication and contribution to synaptic plasticity or maintenance of myelination have been described before.[23,56,57] EVs are also reported to have a role in pathogenesis of neurodegenerative diseases, among others, by transporting and spreading pathological proteins.[30–32] Particularly with regard to the known seeding effect of pathological α-syn,[44,45] its distribution via EVs is of crucial importance. Recent studies detected EVs and NEs in blood and other body fluids *in vivo* and demonstrated their potential as source of biomarkers for neurodegenerative diseases.[23,24,57–59] In our study, we confirmed the presence of EVs by immunoblotting, DLS measurements and TEM imaging (Fig. 1 and Supplementary Fig. 1). In dot blot and western blot analyses, a strong signal intensity of the EV markers CD63, CD9 and CD81 were detected (Fig. 1B and C and Supplementary Fig. 2A–C, E and F). Also, size distribution (30–100 nm) and morphology of EVs were typical (Fig. 1D and E and Supplementary Fig. 1D and E).[60]

So far, the most common method to isolate EVs still contain plasma proteins and protein aggregates, which has been discussed as limiting factor for the diagnostic evaluation.[53,61,62] Hence, for a more specific analysis, we used an immune-affinity capturing protocol and precipitated EVs positive for the neuronal cell adhesion molecule L1 (NCAM-L1) from all plasma-derived EVs. NCAM-L1 is also known as a specific surface marker of NEs.[58,63,64] Interestingly, a recent study by Norman *et al.*[65] used density gradient centrifugation and size-exclusion chromatography to separate EVs from soluble proteins and found that NCAM-L1 was primarily detected in the soluble protein fraction, but supposedly not in the EV-derived protein fractions. In contrast to the protocol of Norman *et al.*[65] that separated NCAM-L1 directly from the plasma samples, we first isolated the total of EVs from plasma samples and extracted in a next step NEs from these EVs. In this way, we avoided the potential contamination through the soluble NCAM-L1 fraction. Discrepancies between our study and the work of Norman *et al.*[65] might therefore be explained by the different protocols. Importantly, the presence of intact NEs was confirmed by the presence of neuron-derived vesicles through immunoblotting, DLS measurement and TEM analysis (Fig. 2 and Supplementary Fig. 2). Moreover, high levels of neuronal proteins (including synaptophysin, neuron-specific enolase, protein gene product 9.5 and α-syn) as well as the EV markers CD63, CD9 and CD81 could be detected, underlining the presence of NEs after precipitation via NCAM-L1 (Fig. 2B–D and Supplementary Fig. 2A–C and E–H). Likewise, other studies confirmed the presence of NCAM-L1 on EVs and demonstrate its neuronal cargo.[24,66–69] Determining the concentration of plasma-derived EVs and the portion of corresponding NEs, we were able to calculate a fraction of 2–6% NEs of all EVs to belong to the NE-pool of vesicles with no significant differences in concentrations of NEs between Parkinson's disease samples and controls. For both, total EVs and its subgroup NEs, we were able to verify their isolation by immunoblot as well as TEM and show by DLS measurements the presence of particles in the size of EVs (Figs 1D, E, 2E and F and Supplementary Fig. 1D, E and 2I and J). Our data further indicates no significant difference in the size and number of EVs as well

as NEs in Parkinson's disease patients versus controls (Figs 1E and 2F and Supplementary Figs 1E and 2J), indicating that the pathophysiological processes in Parkinson's disease do not alter the homeostasis and secretion of EVs and NEs.

To get further insights in Parkinson's disease-associated changes in NE-cargo, we evaluated α-syn levels within the soluble protein fraction of NEs from Parkinson's disease patients and controls (Fig. 3A and B and Supplementary Fig. 3A). For both groups, we could detect similar total α-syn levels by immunoblotting (utilized α-syn antibodies: Syn-1, C20). For western blot analyses, samples were reduced and denatured, resulting in an α-syn signal corresponding to its monomeric size (~16 kDa). On the one hand, other studies demonstrated no robust α-syn distribution in plasma samples of Parkinson's disease patients and control subjects.[24,52,70] On the other hand, they indicated increased α-syn levels in EVs/NEs in Parkinson's disease patients using ELISA and Luminex assays or mass spectrometry and multiplexed electrochemiluminescence compared to healthy controls.[24,59,71,72] In a recent study, Stuendl *et al.*[72] demonstrated a significant increase in α-syn concentration of plasma-derived EVs (ratio of EV-α-syn to EV particle number) from Parkinson's disease patients in comparison to the control group and other Parkinsonian syndromes. However, in the validation cohort of patients less pronounced differences between Parkinson's disease patients and other Parkinsonian syndromes were found.[72] Moreover, in another study the decreased EV particle number described by Stuendl *et al.*,[72] which codetermined the α-syn concentration, was not seen.[73] The group of Jiang *et al.*[71] also analysed NEs and showed increased α-syn levels in prodromal and clinical Parkinson's disease cohorts using mass spectrometry or multiplexed electrochemiluminescence. In a more recent publication, they validated their findings and were able to distinguish the Parkinson's disease cohort from patients with a glial synucleinopathy or tauopathy.[74] Interestingly, opposite findings were described by Si *et al.*,[75] depicting decreased α-syn levels in NEs of Parkinson's disease patients compared to controls using ELISA.[75] These contradictory results could be due to different methods and protocols as well as the inconsistent use of EVs or NEs. As we based our study on the detection of pathological α-syn conformers rather than on the concentration of α-syn, we offer a methodological approach that is clearly pathology-related and less vulnerable to the methodological differences. We therefore find this strategy promising for the identification of Parkinson's disease patients.

Another important point in our protocol is the separation between soluble and insoluble protein fractions of NE lysates. Only the soluble supernatant was further analysed by subsequent biochemical analyses, as soluble α-syn oligomeric conformers have been suggested to mediate α-syn aggregation and convey neurotoxicity.[76–79] Hence, our analyses include immunoblotting of the soluble fraction under native conditions (non-denatured) using a conformation-specific α-syn antibody (MJFR-14-6-4-2), binding to oligomeric and filamentous α-syn species (Fig. 3C).[43,80] Applying this protocol, we could demonstrate the presence of soluble α-syn conformers in all Parkinson's disease patient-NE samples.

The MJFR signal intensity was significantly increased in Parkinson's disease samples compared to control NEs, separating Parkinson's disease and control group (Fig. 3D and E), as also confirmed by the OC antibody,[81] that interacts with amyloid oligomers (Fig. 3F and G). This result offers the potential to establish a reliable diagnostic assay on the basis of structural properties of soluble α-syn fractions. Although ELISAs are quantitative, dot blot analyses serve as a proof of concept to specifically detect pathological α-syn conformers without using technically complex methods. By using dot blot analyses, we were able to detect pathological soluble α-syn species in the nanogram range (Supplementary Fig. 3E). Taken together, our findings are based on a strict sequence and essential combination of experimental steps containing the isolation of NEs and subsequent analysis of the soluble fraction under native conditions with a structure-specific antibody (Fig. 3C). Importantly, no differences in total α-syn levels (Syn-1 antibody, C20 antibody) could be observed, when performing dot blot or western blot analyses of the soluble protein fraction (Fig. 3A, B, H and I). Accordingly, our data suggest no increase in total, soluble α-syn in Parkinson's disease patients, but a shift towards pathology-associated oligomeric/filamentous conformers (Fig. 3C).

In addition, we used an adjusted α-syn seeding assay to analyse the seeding potential of the EV- and NE-derived α-syn species extracted from the soluble protein fraction of the vesicles. Our findings demonstrate that it is possible to amplify α-syn species from blood-derived EVs/NEs of Parkinson's disease patients. This is not only important for understanding the role of vesicular α-syn in disease pathology, but also for amplification of this α-syn conformer for subsequent structural analyses, which is discussed next. In contrast to other seeding assays, we used less substrate (recombinant monomeric α-syn) and obtained lower ThT values accordingly.[17,44] Still, specific and significant increases in fluorescence could be measured as indicated by using respective controls. Moreover, we could illustrate the superior seeding capacity of NEs compared to plasma or EVs (Fig. 4). These results are further underlined by comparing MJFR antibody signal intensities after seeding assay (Fig. 4I). Whereas plasma samples did not show any significant differences between Parkinson's disease patients and controls before and after seeding, EVs and NEs exhibited substantial increases in MJFR signal intensities in samples obtained from Parkinson's disease patients in comparison to controls (Fig. 4C, F and I). Overall, NEs derived from Parkinson's disease patients exhibited the strongest MJFR signal intensities as well as the strongest seeding capacity presumably constituted by their direct CNS origin. This suggests NEs could be considered an ideal matrix for the investigation of brain-associated pathologies.[32,59,82,83]

Amplification of NE-derived α-syn by seeding assay allowed further structural characterization by biophysical and biochemical analyses. Taken together, our data revealed β-sheet rich conformations and a fibril-like organization of NE-derived α-syn from Parkinson's disease patients. We could further demonstrate that this α-syn conformer transforms into fibrillary structures of higher orders as indicated by TEM analyses (Fig. 5B). SDS–PAGE and following silver staining of seeding assay end products confirmed the size of monomeric α-syn, as part of the formed aggregates (Supplementary Fig. 5B). Compared to other α-syn species described in Parkinson's disease patients, our findings demonstrate a similar structural constitution as pathological α-syn derived from CSF or the brain of Parkinson's disease patients.[17,84] Since the constitution of α-syn conformers determines its seeding capacities, cellular toxic effects[85] and thus potentially the disease cause,[17] it is important to solve its structure to an ultrastructural level. Hence, studies applying cryo-TEM analyses[86] of the NE-derived α-syn conformer will be part of a future study.

We consider this study as a proof of concept to identify pathological α-syn species in the plasma of Parkinson's disease patients, which are not detectable in controls. To the best of our knowledge, the protocol described here offers the development of a biochemical blood-based test for the diagnosis of Parkinson's disease that involves the pathological hallmark of Parkinson's disease, i.e. misfolded of α-syn.

Additional studies will need to validate this protocol in a blinded fashion in larger cohorts. Moreover, it will be important to compare the NE-derived α-syn species to α-syn conformers derived from brain tissue and CSF of Parkinson's disease patients. Consequently, further investigations will be necessary to confirm our findings in different stages of Parkinson's disease and to evaluate whether NE-derived α-syn may serve as progression marker or is even detectable in the very early prodromal-stages, like in patients with polysomnographically confirmed rapid eye movement sleep behaviour disorder. In addition, a larger cohort of control subjects, that reflects the general population, is needed for the validation of the demonstrated protocol. Also, plasma samples of other α-synucleinopathies including samples of patients with dementia with Lewy bodies and multiple system atrophy will need to be investigated to elaborate possible similarities or differences between these disease entities. Next steps should also include approaches to foster the development of methods, which will enable standardized measurements of much larger sample pools making this approach applicable for the clinical routine.

Conclusion

In summary, we demonstrate that pathological soluble α-syn conformers detected in blood plasma-derived NEs can serve as a biomarker to differentiate Parkinson's disease patients from healthy controls. Further confirmation of the presence of pathological soluble α-syn conformers was reached by amplification and ultrastructural analysis of the formed aggregates. Our study supports the approach that instead of focusing on quantitative α-syn level in body fluids or tissues, the detection of pathological neuronal α-syn conformers should be targeted.

Acknowledgements

We sincerely thank Professor Dr Stefan Rose-John and Professor Dr Paul Saftig for providing support and infrastructure. Moreover, we thank Melanie Boss for excellent technical assistance. We also gratefully acknowledge the commitment of patients and control individuals in participating and donating blood samples.

Funding

This work was supported by the following grants: ParkinsonFonds Germany to D.B., F.Z.; Deutsche Forschungsgemeinschaft (DFG, German Research Foundation), grant number 125440785 – SFB 877, B11 to F.Z.

Competing interests

The authors report no competing interests.

Supplementary material

Supplementary material is available at *Brain* online.

References

1. Braak H, Del Tredici K, Rüb U, de Vos RA, Jansen Steur EN, Braak E. Staging of brain pathology related to sporadic Parkinson's disease. *Neurobiol Aging*. 2003;24:197–211.
2. Postuma RB, Poewe W, Litvan I, *et al*. Validation of the MDS clinical diagnostic criteria for Parkinson's disease. *Mov Disord*. 2018; 33:1601–1608.
3. Hughes AJ, Daniel SE, Kilford L, Lees AJ. Accuracy of clinical diagnosis of idiopathic Parkinson's disease: A clinico-pathological study of 100 cases. *J Neurol Neurosurg Psychiatry*. 1992;55: 181–184.
4. Jain S, Lo SE, Louis ED. Common misdiagnosis of a common neurological disorder: How are we misdiagnosing essential tremor? *Arch Neurol*. 2006;63:1100–1104.
5. Newman EJ, Breen K, Patterson J, Hadley DM, Grosset KA, Grosset DG. Accuracy of Parkinson's disease diagnosis in 610 general practice patients in the West of Scotland. *Mov Disord*. 2009;24:2379–2385.
6. Schrag A, Ben-Shlomo Y, Quinn N. How valid is the clinical diagnosis of Parkinson's disease in the community? *J Neurol Neurosurg Psychiatry*. 2002;73:529–534.
7. Riederer P, Berg D, Casadei N, *et al*. α-Synuclein in Parkinson's disease: Causal or bystander? *J Neural Transm (Vienna)*. 2019; 126:815–840.
8. Atik A, Stewart T, Zhang J. Alpha-synuclein as a biomarker for Parkinson's disease. *Brain Pathol*. 2016;26:410–418.
9. Beach TG, Corbille AG, Letournel F, *et al*. Multicenter assessment of immunohistochemical methods for pathological alpha-synuclein in sigmoid colon of autopsied Parkinson's disease and control subjects. *J Parkinsons Dis*. 2016;6:761–770.
10. Bloch A, Probst A, Bissig H, Adams H, Tolnay M. Alpha-synuclein pathology of the spinal and peripheral autonomic nervous system in neurologically unimpaired elderly subjects. *Neuropathol Appl Neurobiol*. 2006;32:284–295.
11. Manne S, Kondru N, Jin H, *et al*. Blinded RT-QuIC analysis of α-synuclein biomarker in skin tissue from Parkinson's disease patients. *Mov Disord*. 2020;35:2230–2239.
12. Beach TG, Adler CH, Sue LI, *et al*. Multi-organ distribution of phosphorylated α-synuclein histopathology in subjects with Lewy body disorders. *Acta Neuropathol*. 2010;119:689–702.
13. Ma LY, Liu GL, Wang DX, Zhang MM, Kou WY, Feng T. Alpha-synuclein in peripheral tissues in Parkinson's disease. *ACS Chem Neurosci*. 2019;10:812–823.
14. Schaeffer E, Kluge A, Böttner M, *et al*. Alpha synuclein connects the gut-brain axis in Parkinson's disease patients - A view on clinical aspects, cellular pathology and analytical methodology. *Front Cell Dev Biol*. 2020;8:573696.
15. Wang Z, Becker K, Donadio V, *et al*. Skin α-synuclein aggregation seeding activity as a novel biomarker for Parkinson disease. *JAMA Neurol*. 2020;78:1–11.
16. Chahine LM, Beach TG, Brumm MC, *et al*. *In vivo* distribution of α-synuclein in multiple tissues and biofluids in Parkinson disease. *Neurology*. 2020;95:e1267–e1284.
17. Shahnawaz M, Mukherjee A, Pritzkow S, *et al*. Discriminating α-synuclein strains in Parkinson's disease and multiple system atrophy. *Nature*. 2020;578:273–277.
18. Mehta SH, Adler CH. Advances in biomarker research in Parkinson's disease. *Curr Neurol Neurosci Rep*. 2016;16:7.
19. Lee PH, Lee G, Park HJ, Bang OY, Joo IS, Huh K. The plasma alpha-synuclein levels in patients with Parkinson's disease and multiple system atrophy. *J Neural Transm (Vienna)*. 2006;113: 1435–1439.
20. Foulds PG, Mitchell JD, Parker A, *et al*. Phosphorylated α-synuclein can be detected in blood plasma and is potentially a useful biomarker for Parkinson's disease. *FASEB J*. 2011;25: 4127–4137.
21. Li QX, Mok SS, Laughton KM, *et al*. Plasma α-synuclein is decreased in subjects with Parkinson's disease. *Exp Neurol*. 2007; 204:583–588.

22. El-Agnaf OM, Salem SA, Paleologou KE, *et al*. Detection of oligomeric forms of α-synuclein protein in human plasma as a potential biomarker for Parkinson's disease. *FASEB J*. 2006;20:419–425.
23. Budnik V, Ruiz-Cañada C, Wendler F. Extracellular vesicles round off communication in the nervous system. *Nat Rev Neurosci*. 2016;17:160–172.
24. Shi M, Liu C, Cook TJ, *et al*. Plasma exosomal α-synuclein is likely CNS-derived and increased in Parkinson's disease. *Acta Neuropathol*. 2014;128:639–650.
25. Niu M, Li Y, Li G, *et al*. A longitudinal study on α-synuclein in plasma neuronal exosomes as a biomarker for Parkinson's disease development and progression. *Eur J Neurol*. 2020;27:967–974.
26. Shi M, Sheng L, Stewart T, Zabetian CP, Zhang J. New windows into the brain: Central nervous system-derived extracellular vesicles in blood. *Prog Neurobiol*. 2019;175:96–106.
27. Matsumoto J, Stewart T, Sheng L, *et al*. Transmission of α-synuclein-containing erythrocyte-derived extracellular vesicles across the blood-brain barrier via adsorptive mediated transcytosis: Another mechanism for initiation and progression of Parkinson's disease? *Acta Neuropathol Commun*. 2017;5:71.
28. Alvarez-Erviti L, Seow Y, Yin H, Betts C, Lakhal S, Wood MJ. Delivery of siRNA to the mouse brain by systemic injection of targeted exosomes. *Nat Biotechnol*. 2011;29:341–345.
29. Matsumoto J, Stewart T, Banks WA, Zhang J. The transport mechanism of extracellular vesicles at the blood-brain barrier. *Curr Pharm Design*. 2017;23:6206–6214.
30. Grey M, Dunning CJ, Gaspar R, *et al*. Acceleration of α-synuclein aggregation by exosomes. *J Biol Chem*. 2015;290:2969–2982.
31. Emmanouilidou E, Melachroinou K, Roumeliotis T, *et al*. Cell-produced alpha-synuclein is secreted in a calcium-dependent manner by exosomes and impacts neuronal survival. *J Neurosci*. 2010;30:6838–6851.
32. Coleman BM, Hill AF. Extracellular vesicles–Their role in the packaging and spread of misfolded proteins associated with neurodegenerative diseases. *Semin Cell Dev Biol*. 2015;40:89–96.
33. Théry C, Witwer KW, Aikawa E, *et al*. Minimal information for studies of extracellular vesicles 2018 (MISEV2018): A position statement of the International Society for Extracellular Vesicles and update of the MISEV2014 guidelines. *J Extracell Vesicles*. 2018;7:1535750.
34. Zunke F, Moise AC, Belur NR, *et al*. Reversible conformational conversion of α-synuclein into toxic assemblies by glucosylceramide. *Neuron*. 2018;97:92–107.e10.
35. Xiang W, Menges S, Schlachetzki JC, *et al*. Posttranslational modification and mutation of histidine 50 trigger alpha synuclein aggregation and toxicity. *Mol Neurodegener*. 2015;10:8.
36. Paleologou KE, Schmid AW, Rospigliosi CC, *et al*. Phosphorylation at Ser-129 but not the phosphomimics S129E/D inhibits the fibrillation of α-synuclein. *J Biol Chem*. 2008;283:16895–905.
37. Eymsh B, Drobny A, Heyn TR, *et al*. Toxic metamorphosis-how changes from lysosomal to cytosolic pH modify the alpha-synuclein aggregation pattern. *Biomacromolecules*. 2020;21:4673–4684.
38. Arnold P, Himmels P, Weiß S, *et al*. Antigenic and 3D structural characterization of soluble X4 and hybrid X4-R5 HIV-1 Env trimers. *Retrovirology*. 2014;11:42.
39. Lückstädt W, Bub S, Koudelka T, *et al*. Cell surface processing of CD109 by Meprin β leads to the release of soluble fragments and reduced expression on extracellular vesicles. *Front Cell Dev Biol*. 2021;9:622390.
40. Sun B, Dalvi P, Abadjian L, Tang N, Pulliam L. Blood neuron-derived exosomes as biomarkers of cognitive impairment in HIV. *Aids*. 2017;31:F9–F17.
41. Nekludov M, Bellander BM, Gryth D, Wallen H, Mobarrez F. Brain-derived microparticles in patients with severe isolated TBI. *Brain Inj*. 2017;31:1856–1862.
42. Goetzl EJ, Elahi FM, Mustapic M, *et al*. Altered levels of plasma neuron-derived exosomes and their cargo proteins characterize acute and chronic mild traumatic brain injury. *FASEB J*. 2019;33:5082–5088.
43. Kumar ST, Jagannath S, Francois C, Vanderstichele H, Stoops E, Lashuel HA. How specific are the conformation-specific α-synuclein antibodies? Characterization and validation of 16 alpha-synuclein conformation-specific antibodies using well-characterized preparations of α-synuclein monomers, fibrils and oligomers with distinct structures and morphology. *Neurobiol Dis*. 2020;146:105086.
44. Paciotti S, Bellomo G, Gatticchi L, Parnetti L. Are we ready for detecting α-synuclein prone to aggregation in patients? The case of 'protein-misfolding cyclic amplification' and 'Real-time quaking-induced conversion' as diagnostic tools. *Front Neurol*. 2018;9:415.
45. Shahnawaz M, Tokuda T, Waragai M, *et al*. Development of a biochemical diagnosis of Parkinson disease by detection of α-synuclein misfolded aggregates in cerebrospinal fluid. *JAMA Neurol*. 2017;74:163–172.
46. Mollenhauer B, Cullen V, Kahn I, *et al*. Direct quantification of CSF alpha-synuclein by ELISA and first cross-sectional study in patients with neurodegeneration. *Exp Neurol*. 2008;213:315–325.
47. Tokuda T, Salem SA, Allsop D, *et al*. Decreased α-synuclein in cerebrospinal fluid of aged individuals and subjects with Parkinson's disease. *Biochem Biophys Res Commun*. 2006;349:162–166.
48. Hong Z, Shi M, Chung KA, *et al*. DJ-1 and α-synuclein in human cerebrospinal fluid as biomarkers of Parkinson's disease. *Brain*. 2010;133:713–726.
49. Mollenhauer B, Parnetti L, Rektorova I, *et al*. Biological confounders for the values of cerebrospinal fluid proteins in Parkinson's disease and related disorders. *J Neurochem*. 2016;139:290–317.
50. Eusebi P, Giannandrea D, Biscetti L, *et al*. Diagnostic utility of cerebrospinal fluid α-synuclein in Parkinson's disease: A systematic review and meta-analysis. *Mov Disord*. 2017;32:1389–1400.
51. Gao L, Tang H, Nie K, *et al*. Cerebrospinal fluid alpha-synuclein as a biomarker for Parkinson's disease diagnosis: A systematic review and meta-analysis. *Int J Neurosci*. 2015;125:645–654.
52. Shi M, Zabetian CP, Hancock AM, *et al*. Significance and confounders of peripheral DJ-1 and alpha-synuclein in Parkinson's disease. *Neurosci Lett*. 2010;480:78–82.
53. Xu R, Greening DW, Zhu HJ, Takahashi N, Simpson RJ. Extracellular vesicle isolation and characterization: Toward clinical application. *J Clin Invest*. 2016;126:1152–1162.
54. Simpson RJ, Lim JW, Moritz RL, Mathivanan S. Exosomes: Proteomic insights and diagnostic potential. *Expert Rev Proteomics*. 2009;6:267–283.
55. Fujita Y, Yoshioka Y, Ochiya T. Extracellular vesicle transfer of cancer pathogenic components. *Cancer Sci*. 2016;107:385–390.
56. Yáñez-Mó M, Siljander PR, Andreu Z, *et al*. Biological properties of extracellular vesicles and their physiological functions. *J Extracell Vesicles*. 2015;4:27066.
57. Lee TH, D'Asti E, Magnus N, Al-Nedawi K, Meehan B, Rak J. Microvesicles as mediators of intercellular communication in cancer–The emerging science of cellular 'debris'. *Semin Immunopathol*. 2011;33:455–467.
58. Simpson RJ, Kalra H, Mathivanan S. ExoCarta as a resource for exosomal research. *J Extracell Vesicles*. 2012:1.
59. Zhao ZH, Chen ZT, Zhou RL, Zhang X, Ye QY, Wang YZ. Increased DJ-1 and α-synuclein in plasma neural-derived

exosomes as potential markers for Parkinson's disease. *Front Aging Neurosci*. 2018;10:438.
60. Momen-Heravi F, Balaj L, Alian S, *et al*. Alternative methods for characterization of extracellular vesicles. *Front Physiology*. 2012;3:354.
61. Mateescu B, Kowal EJ, van Balkom BW, *et al*. Obstacles and opportunities in the functional analysis of extracellular vesicle RNA - An ISEV position paper. *J Extracell Vesicles*. 2017;6:1286095.
62. Sódar BW, Kittel Á, Pálóczi K, *et al*. Low-density lipoprotein mimics blood plasma-derived exosomes and microvesicles during isolation and detection. *Sci Rep*. 2016;6:24316.
63. Fauré J, Lachenal G, Court M, *et al*. Exosomes are released by cultured cortical neurones. *Mol Cell Neurosci*. 2006;31:642–648.
64. Kenwrick S, Watkins A, De Angelis E. Neural cell recognition molecule L1: Relating biological complexity to human disease mutations. *Hum Mol Genet*. 2000;9:879–886.
65. Norman M, Ter-Ovanesyan D, Trieu W, *et al*. L1CAM is not associated with extracellular vesicles in human cerebrospinal fluid or plasma. *Nat Methods*. 2021;18:631–634.
66. Mustapic M, Eitan E, Werner JK, Jr., *et al*. Plasma extracellular vesicles enriched for neuronal origin: A potential window into brain pathologic processes. *Front Neurosci*. 2017;11:278.
67. Shi M, Kovac A, Korff A, *et al*. CNS tau efflux via exosomes is likely increased in Parkinson's disease but not in Alzheimer's disease. *Alzheimer's & Dementia*. 2016;12:1125–1131.
68. Winston CN, Goetzl EJ, Akers JC, *et al*. Prediction of conversion from mild cognitive impairment to dementia with neuronally derived blood exosome protein profile. *Alzheimer's & Dement (Amst)*. 2016;3:63–72.
69. Kapogiannis D, Mustapic M, Shardell MD, *et al*. Association of extracellular vesicle biomarkers with Alzheimer disease in the Baltimore longitudinal study of aging. *JAMA Neurol*. 2019;76:1340–1351.
70. Foulds PG, Diggle P, Mitchell JD, *et al*. A longitudinal study on α-synuclein in blood plasma as a biomarker for Parkinson's disease. *Sci Rep*. 2013;3:2540.
71. Jiang C, Hopfner F, Katsikoudi A, *et al*. Serum neuronal exosomes predict and differentiate Parkinson's disease from atypical parkinsonism. *J Neurol Neurosurg Psychiatry*. 2020;91:720–729.
72. Stuendl A, Kraus T, Chatterjee M, *et al*. α-Synuclein in plasma-derived extracellular vesicles is a potential biomarker of Parkinson's disease. *Mov Disord*. 2021;36:2508–2518.
73. Cerri S, Ghezzi C, Sampieri M, *et al*. The exosomal/total α-synuclein ratio in plasma is associated with glucocerebrosidase activity and correlates with measures of disease severity in PD patients. *Front Cell Neurosci*. 2018;12:125.
74. Jiang C, Hopfner F, Berg D, *et al*. Validation of α-synuclein in L1CAM-immunocaptured exosomes as a biomarker for the stratification of Parkinsonian syndromes. *Mov Disord*. 2021;36:2663–2669.
75. Si X, Tian J, Chen Y, Yan Y, Pu J, Zhang B. Central nervous system-derived exosomal alpha-synuclein in serum may be a biomarker in Parkinson's disease. *Neuroscience*. 2019;413:308–316.
76. Kayed R, Head E, Thompson JL, *et al*. Common structure of soluble amyloid oligomers implies common mechanism of pathogenesis. *Science*. 2003;300:486–489.
77. Fusco G, Chen SW, Williamson PTF, *et al*. Structural basis of membrane disruption and cellular toxicity by α-synuclein oligomers. *Science*. 2017;358:1440–1443.
78. Chen SW, Drakulic S, Deas E, *et al*. Structural characterization of toxic oligomers that are kinetically trapped during α-synuclein fibril formation. *Proc Natl Acad Sci USA*. 2015;112:E1994–E2003.
79. Mor DE, Tsika E, Mazzulli JR, *et al*. Dopamine induces soluble α-synuclein oligomers and nigrostriatal degeneration. *Nat Neurosci*. 2017;20:1560–1568.
80. Lassen LB, Gregersen E, Isager AK, Betzer C, Kofoed RH, Jensen PH. ELISA method to detect α-synuclein oligomers in cell and animal models. *PLoS ONE*. 2018;13:e0196056.
81. Kayed R, Head E, Sarsoza F, *et al*. Fibril specific, conformation dependent antibodies recognize a generic epitope common to amyloid fibrils and fibrillar oligomers that is absent in prefibrillar oligomers. *Mol Neurodegener*. 2007;2:18.
82. Thompson AG, Gray E, Heman-Ackah SM, *et al*. Extracellular vesicles in neurodegenerative disease - Pathogenesis to biomarkers. *Nat Rev Neurol*. 2016;12:346–357.
83. Yuyama K, Sun H, Mitsutake S, Igarashi Y. Sphingolipid-modulated exosome secretion promotes clearance of amyloid-β by microglia. *J Biol Chem*. 2012;287:10977–10989.
84. Van der Perren A, Gelders G, Fenyi A, *et al*. The structural differences between patient-derived α-synuclein strains dictate characteristics of Parkinson's disease, multiple system atrophy and dementia with Lewy bodies. *Acta Neuropathol*. 2020;139:977–1000.
85. Peng C, Gathagan RJ, Covell DJ, *et al*. Cellular milieu imparts distinct pathological α-synuclein strains in α-synucleinopathies. *Nature*. 2018;557:558–563.
86. Guerrero-Ferreira R, Taylor NM, Arteni AA, *et al*. Two new polymorphic structures of human full-length alpha-synuclein fibrils solved by cryo-electron microscopy. *eLife*. 2019:8.